Supporting Information For:

Modest Effects of Lipid Modifications on the Structure of Caveolin-3

Ji-Hun Kim, Dungeng Peng, Jonathan P. Schlebach, Arina Hadziselimovic, and Charles R. Sanders*

Department of Biochemistry and Center for Structural Biology, Vanderbilt University School of Medicine, Nashville, TN 37232, United States

Contents:

Materials and Methods

Cloning and Plasmid Construction

The cDNA of human Cav-3 was amplified by polymerase chain reaction (PCR), and the cDNA was ligated into a pET16b vector using two restriction endonuclease sites, *Nco I* and *BamH1*. The final pET16b vector contained an N-terminal histidine purification tag, MGHHHHHHG-, to facilitate purification.

Recombinant Expression of Cav3 in E. coli

Vectors were transformed into *E. coli* Rosetta2(DE3) cells, variants of the BL21 strain commonly used for high level protein expression. 20 µl of the transformed culture was plated on LB-agar containing ampicillin and chloramphenicol prior to overnight incubation at 37 °C. A single colony was used to inoculate a starter culture of LB medium containing 100 µg/mL ampicillin and 50 ug/ml chloramphenicol. The starter culture was grown for 10 h at 37 °C. 1.5 mL of this culture was used to

seed 1 L of M9 minimal medium culture, which contained ampicillin, chloramphenicol, glucose, MEM vitamins, 0.1 mM $CaCl_2$, 1 mM $MgSO_4$, and $^{15}NH_4Cl$ for isotopic labeling. Large-scale cultures were then grown at room temperature until the OD_{600} reached 0.65-0.75. Protein expression was induced with the addition of 1 mM IPTG to the cultures. Following 24 hours of induction the cells were harvested by centrifugation. Expression of recombinant Cav3 was confirmed both by Western blot using a monoclonal anti-5X His mouse antibody (Cell Signaling Technology, Danvers, MA) and by mass spectrometry (of the purified protein, see below).

Purification of Human Cav3

Harvested cells were resuspended in 20ml lysis buffer (75 mM Tris, pH 7.8, 300 mM NaCl) per gram of wet cells. The lysis buffer also contained 2 mM ethylenediaminetetraacetic acid (EDTA), 5 mM magnesium acetate, 2 mg/mL lysozyme, 0.2 mg/mL DNase and RNase, and either 50 μL of protease cocktail inhibitor (Sigma-Aldrich, St. Louis, MO) or 0.2ml of phenylmethylsulfonyl fluoride (PMSF) per gram of cells. The suspension was tumbled for 90 min at room temperature followed by sonication on ice for 5 min with a 50% duty cycle at approximately 57 W using a Misonix sonicator (Farmingdale, NY). Inclusion bodies were pelleted by centrifugation at 20,000 rpm for 30 min using a Beckman-Coulter JA 25.5 rotor (approximately 48,000*g*) (Indianapolis, IN). The inclusion bodies were then solubilized in 20 mL of buffer A (40 mM HEPES pH 7.8 and 300 mM NaCl) containing 3% (v/v) Empigen detergent (Sigma-Aldrich, St. Louis, MO) per gram of cells. The solution was then tumbled at 4°C until the mixture clarified (approximately 2 h) and then centrifuged to remove any remaining insoluble particulates. Ni-NTA resin (1.2 mL/g of cells) was equilibrated with buffer A and then added to the supernatant. The mixture was then tumbled for 1 h at room temperature. The resin was loaded into a chromatography column and sequentially washed with buffer A containing 3% (v/v) Empigen and buffer A containing 40 mM imidazole and 1.5% (v/v) Empigen, which eluted non-His_6-tagged proteins from the resin. Empigen was then exchanged for other detergents by re-equilibrating the column with 12 column volumes of 20 mM sodium phosphate (pH 7.2) containing either 0.5% β-n-decylmaltoside (DM), 0.5% dodecylphosphocholine (DPC), 0.2% n-tridecylphosphocholine (Fos-

13), 0.2% n-tetradecylphosphocholine (TDPC), 0.2% lyso-lauroylphosphatidylcholine (LLPC), 0.2% lyso-myristoylphosphatidylcholine (LMPC), 0.1% lyso-palmitoylphosphatidylcholine (LPPC), 0.2% lauryldimethylamine oxide (LDAO), 0.1% lyso-myristoylphosphatidylglycerol (LMPG), or 0.1% lyso-palmitoylphosphatidylglycerol (LPPG). Cav-3 was then eluted from the column with 250 mM imidazole (pH 7.8) and 2mM DTT containing the corresponding detergent in the elution buffer. After adjusting the pH by adding acetic acid, the eluted protein was concentrated at 20 °C using a centrifugal concentrator (10 kDa Amicon Ultra 4ml, EMD Millipore).

Mutagenesis of Cav3

Cav3 has nine native cysteine residues, the 5^{th}, 6^{th}, and 8^{th} of which are known to undergo palmitoylation (C106, C116 and C129). In order to facilitate the specific addition of lipid chains to only these sites, the six natively un-modified cysteine residues were mutated to serine or alanine as follows: C19S, C72A, C94A, C98A, C124S and C140S. The cysteine residues located in membrane domain were replaced with Ala and the others with Ser to match the expected local solvent polarity experienced by these residues [1]. Mutant variants were generated by site-directed mutagenesis using the QuikChange site-directed mutagenesis kit.

Lipidation of Cav3

The method used to lipidate Cav3 is outlined in Figure 1. Ellman's reagent (5,5' –dithio-bis-(2-nitrobenzoic acid) (DTNB), a compound commonly used for sulfhydryl quantification [2], was dissolved to a final concentration of 20 mM in 100 mM sodium phosphate buffer (pH 7.2). 1.5 ml of the DTNB solution was mixed with 300-400 µL of a concentrated solution containing 1-2 mg of purified Cav3 in 250 mM imidazole (pH 7.8), 1 mM EDTA and 2 mM DTT. 60ul of a 100 mM EDTA (pH 7.2) stock solution was then added, and the total volume was then adjusted to 3 ml with 20 mM

sodium phosphate (pH 7.2). The final reaction solution typically contained 30-80 μM protein, 10 mM DTNB, and 5 mM EDTA. The mixture was then tumbled for 4 h at room temperature, leading to formation of disulfide bonds between cysteine thiols and thionitrobenzoate (TNB), the latter of which is a high energy leaving group. The sample was then loaded on an Econo-Pac 10DG buffer exchange column of 10 ml bed volume, which was pre-equilibrated with 0.2% LPPG and 25 mM sodium phosphate buffer (pH 7.2). This removes unreacted DNTB as well as free TNB. The TNB-modified protein was eluted in about 4 ml of buffer, as monitored by A_{280}, and octanethiol or tetradecanethiol were added to the elution pool to a final concentration of 10 mM followed by a 5 h incubation. Thionitrobenzoate-activated cysteine thiols of Cav3 reacted with octanethiol to exchange disulfide bonds to link cysteine thiols to octanethiol, releasing the free thiolate form of thionitrobenzoate. The mixture was then tumbled for 1 h with Ni-NTA resin equilibrated in 25 mM sodium phosphate (pH 7.2). The resin was then loaded into a chromatography column and rinsed with 15 column volumes of 25 mM sodium phosphate (pH 7.2) containing 0.2% LPPG to remove free thiols and thiobenzoate. The tri-octylated protein was then eluted from the column with 250 mM imidazole (pH 7.8) containing 0.2% LPPG. The eluted protein was then concentrated using a centrifugal concentrator at 20 °C and exchanged with the final buffer containing 100 mM imidazole (pH 6.5) and 1 mM EDTA. Final NMR samples were prepared by mixing 134 ul of concentrated protein solution (200-400 uM final concentration) with 18ul of D2O and 18ul of a 100mM imidazole (pH 6.5) solution containing 1 mM EDTA and 15 mM DSS (1.5 mM DSS final). The final concentration of protein was determined by measuring the A_{280} and using an extinction coefficient of 30940 $M^{-1}cm^{-1}$.

Far-UV Circular Dichroism (CD)

CD spectra were acquired using a Jasco J-810 spectropolarimeter equipped with a Peltier temperature control. Samples were purified as described above and exchanged into 25 mM sodium phosphate buffer (pH 6.5) containing 100mM NaCl, 0.5mM EDTA, 1mM TCEP and 0.2% LPPG using an Econo-Pac 10DG column (Bio-Rad). TCEP was omitted from the buffer of the lipidated

samples. CD spectra were acquired from 250 to 190 nm at 25°C with a protein concentration of 8.5 uM using a 1 mm path length cuvette. α helical and β strand content was estimated from the CD spectra using the K2D3 algorithm [3].

NMR Spectroscopy

1D proton NMR spectra were assessed in order to determine the final detergent concentration in the samples. The ratio of the integral of detergent alkyl or acyl chain hydrogens to that of the DSS standard was calculated for each sample. To calculate the final detergent concentration, this ratio was then compared to the ratios calculated for a series of reference samples containing 0.1, 0.5, 1, 2.5, 5 and 10% LPPG and 1.5mM DSS. Final LPPG concentrations typically ranged between 3-6%. 2-D $^{1}H,^{15}N$-TROSY NMR spectra [4] were acquired using Bruker 600, 800, or 900 MHz spectrometers equipped with TXI cryoprobes. NMR data were processed with NMRPIPE [5] and analyzed using SPARKY [6].

TCEP titration NMR measurement

To assess the specificity of the perturbations arising from lipidation, the reducing agent TCEP (pH 6.5) was added to the lipidated 568C-Cav3 NMR sample to a final concentration of 10 mM, and ^{1}H-^{15}N HSQC spectra of lipidated 568C Cav3 was recorded following 0 and 34 hours of equilibration.

NMR relaxation analysis

The longitudinal relaxation rate (R1) and the transverse relaxation rate (R2) of backbone ^{15}N nuclei, as well as the heteronuclear NOEs (hetNOE) between amide ^{15}N and ^{1}H nuclei were assessed using established HSQC based NMR pulse sequences [7]. Relaxation experiments were performed at 900 MHz (21.2 Tesla). T1 values were measured from ^{1}H-^{15}N correlation spectra recorded with

relaxation evolution delays of 100, 250, 500, 800, 1200, 2000, 4000, and 8000 ms. A 3.5 s delay was used between scans. T2 values were measured from ^{1}H-^{15}N correlation spectra recorded using relaxation evolution delays of 16, 32, 48, 64, 80, 112, 144 and 192 ms. A delay of 3.5 s was used between scans. The steady state ^{1}H-^{15}N hetNOE values were determined from peak ratios observed between the two spectra, which were collected with or without a pre-saturation of the proton dimension.

Supporting References

[1] O.D. Monera, T.J. Sereda, N.E. Zhou, C.M. Kay, R.S. Hodges. (1995) Relationship of sidechain hydrophobicity and alpha-helical propensity on the stability of the single-stranded amphipathic alpha-helix, J Pept Sci 1, 319-329.

[2] G.L. Ellman (1959) Tissue sulfhydryl groups. Arch Biochem Biophys 82, 70-77.

[3] C. Louis-Jeune, M.A. Andrade-Navarro, C. Perez-Iratxeta (2011). Prediction of protein secondary structure from circular dichroism using theoretically derived spectra. Proteins. Structure, Function, and Bioinformatics 80, 374-382.

[4] D. Nietlispach. (2005) Suppression of anti-TROSY lines in a sensitivity enhanced gradient selection TROSY scheme. J Biomol NMR 31, 161-166.

[5] F. Delaglio, S. Grzesiek, G.W. Vuister, G. Zhu, J. Pfeifer, A. Bax (1995) NMRPipe: a multidimensional spectral processing system based on UNIX pipes, J Biomol NMR 6, 277-293.

[6] T. D. Goddard and D. G. Kneller, SPARKY 3, University of California, San Francisco

[7] L.E. Kay, D.A. Torchia and A. Bax, (1989) Backbone dynamics of proteins as studied by ^{15}N inverse detected heteronuclear NMR spectroscopy: Application to staphylococcal nuclease. *Biochemistry 28*, 8972-8979.

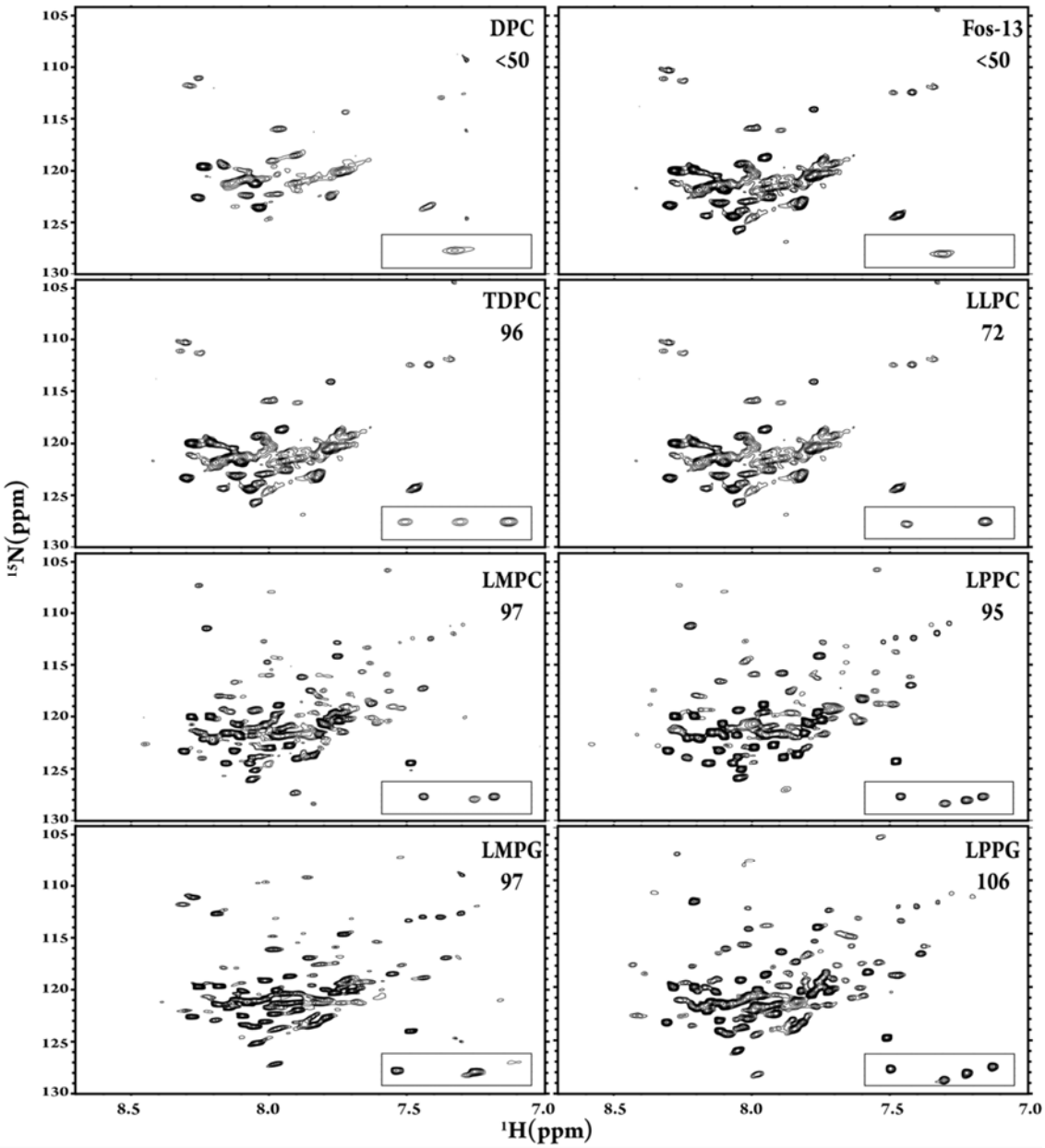

Figure S1. Comparison of the 600 MHz ^{1}H,^{15}N-TROSY spectra of full-length WT Cav3 in various detergent micelles (1mM EDTA, 1mM DTT and 250mM imidazole, pH 6.5, and 318K). The ^{1}H ^{15}N TROSY spectrum of Cav3 in the indicated detergent micelles is shown. The detergent used and the number of resolvable backbone amide peaks is indicated within each panel. The expected number of backbone amides is 153 including N-terminal His tag. The inset panel shows the tryptophan indole peaks. The expected number of tryptophan side chain peaks is 4.

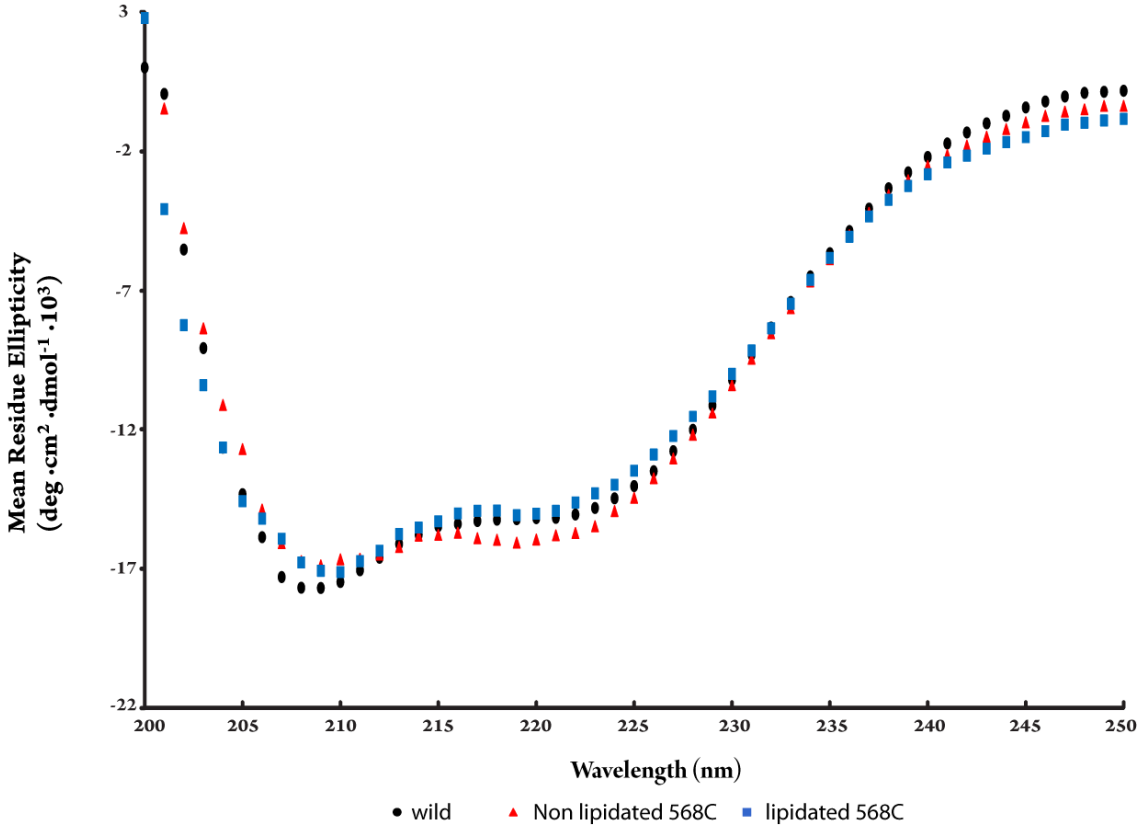

Figure S2. The far-UV Circular Dichroism (CD) spectra of **wild-type (black circles)**, **568C-Cav3 (red triangles)**, and **lipidated 568C-Cav3 (blue squares)** was recorded at 25° C and is plotted against the wavelength in nm. Samples contained LPPG micelles. We then utilized the K2D3 algorithm to assess the secondary structure content of wild-type Cav3 (49 % α helix and 8 % β sheet), 568C-Cav3 (47 % α helix and 10 % β sheet), and lipidated 568C-Cav3 (48 % α helix and 9 % β sheet) suggested by these spectra. The calculated secondary structure is therefore deemed to be the same, within experimental uncertainty, for each construct.

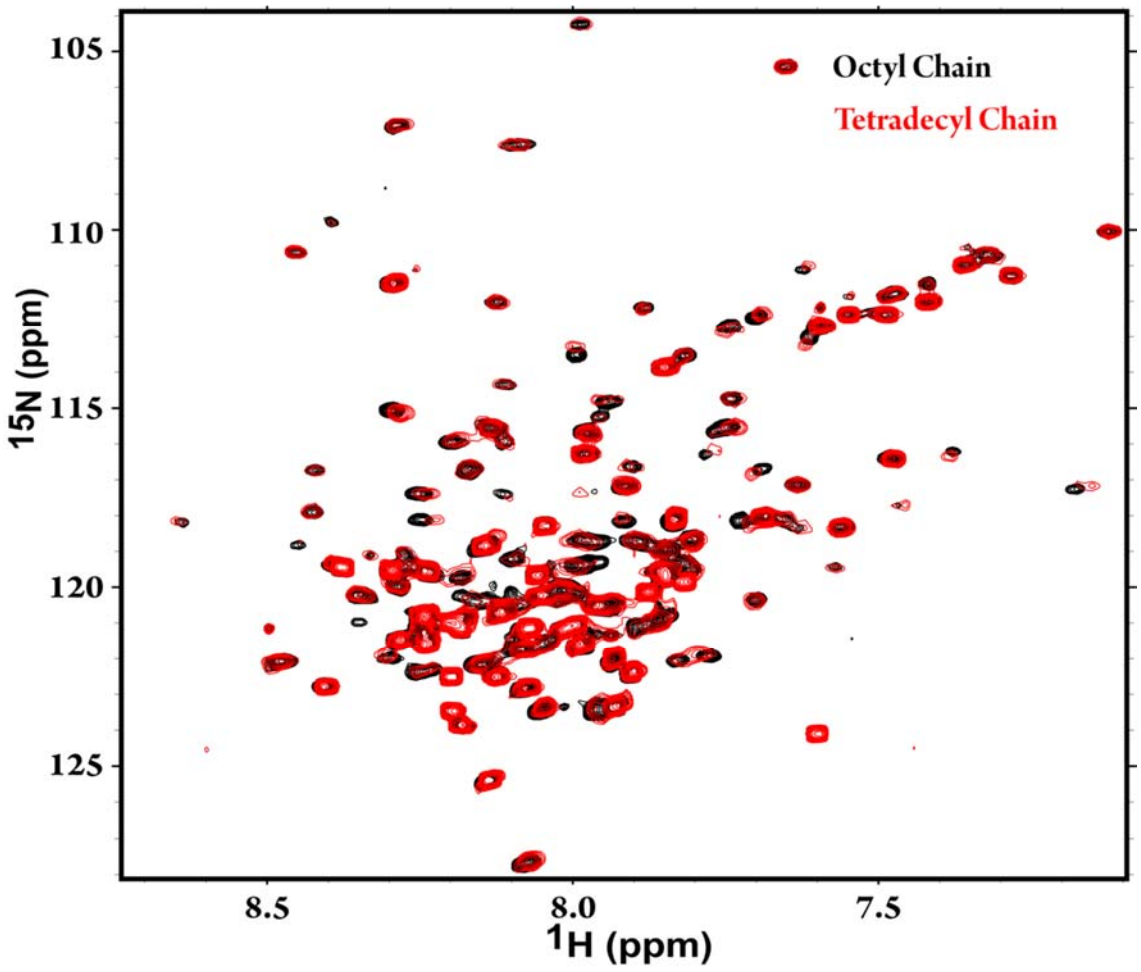

Figure S3. The ^{1}H-^{15}N HSQC spectra of **octylated 568C-Cav3 (black)** and **tetradecylated 568C-Cav3 (red)** are plotted for the sake of comparison.

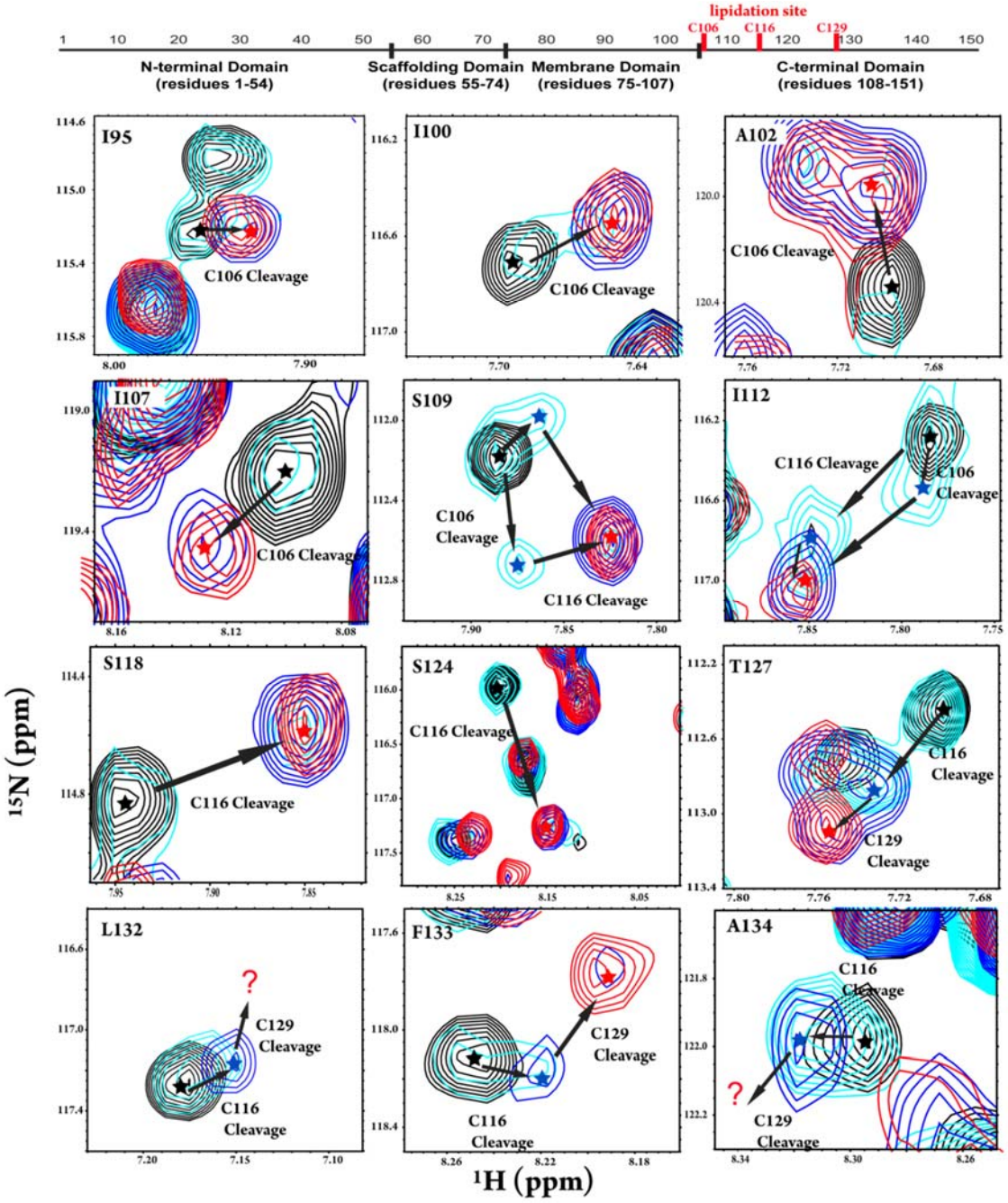

Figure S4. Representative resonances within the ^{1}H-^{15}N HSQC spectra of lipidated (**black**) and non-lipidated 568C-Cav3 (**red**), as well as those of lipidated 568C-Cav3 following equilibration in the presence of 10 mM TCEP (which slowly removes the lipid chains to reveal intermediate states in the de-lipidation pathways). The **cyan** spectrum was collected starting immediately after adding TCEP (but required 5 hours to collect), while the **blue** spectrum (also requiring 5 hours to collect) was acquired starting 34 hours after adding TCEP. The chemical shift perturbations of the resonances of I95, I100, A102, and I107 caused by lipid modifications were

reversed upon equilibration in the presence of TCEP, which is likely due to the reduction of the lipid modification at residue C106. Similar reversions were observed in the resonances corresponding to S109 and I112, though the presence of kinetic intermediates in this case suggest that these perturbations likely caused by multiple lipid modifications (perhaps both modifications at C106 and C116). Reversions of the chemical shifts associated with the resonances of S118 and S124 were apparent and likely correspond to the reduction of the modification at residue C116. Reversion of the chemical shifts associated with the resonances of residues T127, L132, F133 and A134 were apparent, and the position of these residues along with the presence of kinetic intermediates suggests that the perturbations in these residues arise as a result of the modifications at both C116 and C129. The resonances of I132 and A134, which were not present in the spectrum of non-lipidated 568C-Cav3, were shifted after a 34 hr equilibration with TCEP but not completely absent, suggesting the complete reduction of the modification at residue C129 might be quite slow. The peaks for A102 and S118 that correspond to the lipidated and non-lipidated species in the spectrum of lipidated 568C-Cav3 spectra were integrated, and suggest yields of about 88% and 76% for the lipidation of C106 and C116, respectively. Due to the fact that the resonance associated with F133 in the non-lipidated species was not present in the spectrum of lipidated 568C-Cav3, the lipidation of C129 appears to be >90% efficient. Because the total population of incompletely modified protein is minor and contains multiple forms (each with a different combination of lipidated and non-lipidated cysteine residues, each with its own NMR spectrum), the observed spectrum is dominated by the fully-modified species carrying three acyl chain modifications. This makes interpretation of the data in terms of the behavior of the completely lipidated protein straightforward. All spectra were acquired at pH 6.5, 318K and 900MHz.

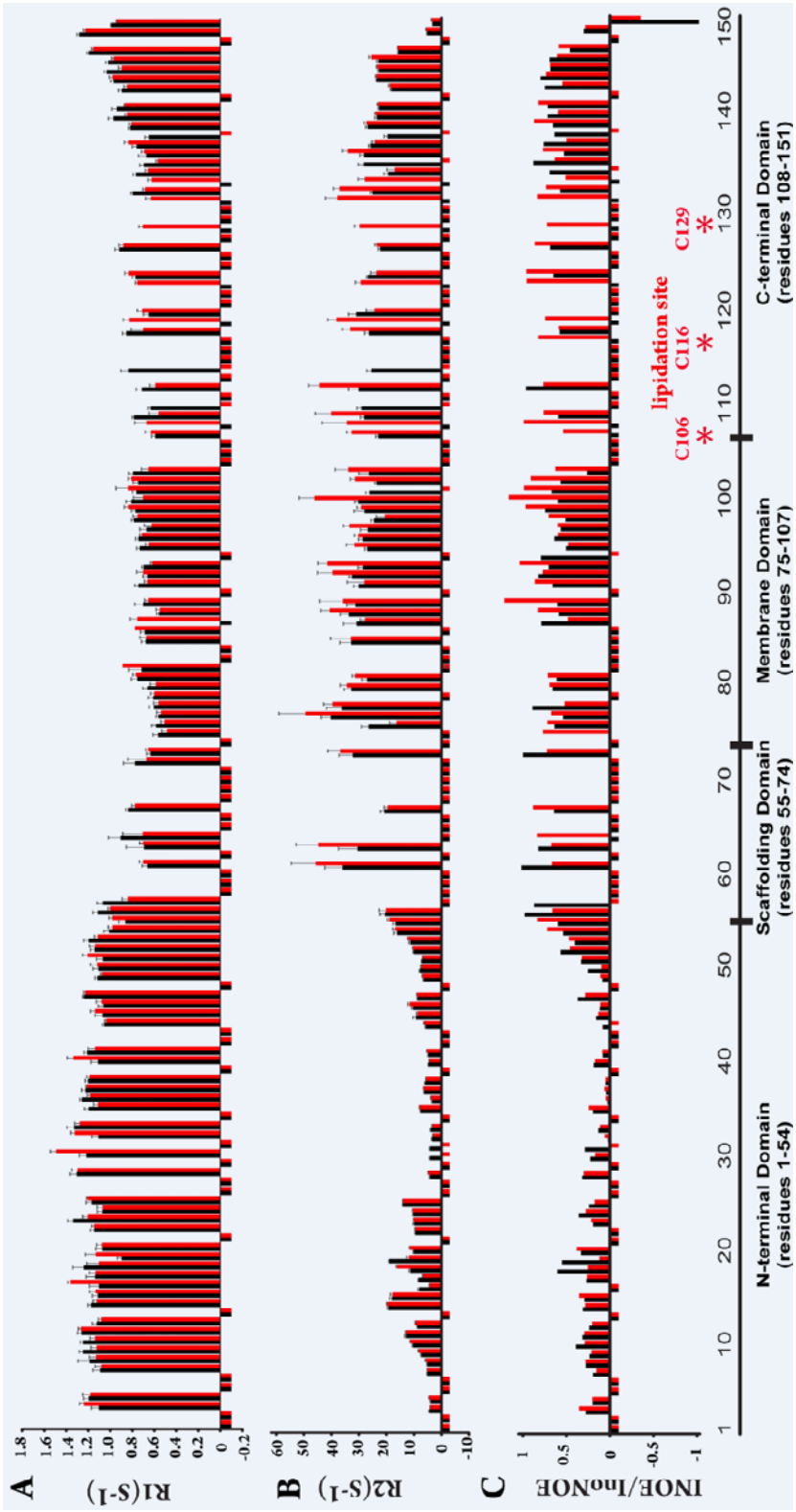

Figure S5. Structural dynamics of Cav3. Site-specific (A) ^{15}N longitudinal relaxation rates (R1), (B) transverse relaxation rates (R2), and (C) steady-state ^{1}H-^{15}N NOEs values of 568C-Cav3 with (**red**) and without (**black**)

lipidation in LPPG micelles at 900 MHz at pH 6.5 and 318K. Negative values indicate residues that could not be assigned due to peak broadening or overlap. The general pattern of R1, R2 and HeteroNOE values from the lipidated and non-lipidated samples are quite similar and are consistent with the expected topology of Cav3, which suggest that lipidation does not significantly alter the global fold of the protein. However, lipidation increases the R2 and HeteroNOE values of the residues near the modification sites and in the proximal end of the membrane domain, which implies the rigidity of this region is enhanced, as a result of anchoring of this region to the micelle surface.